The Complete Spectrum of Image Line

TULLIO ROZZI, SENIOR MEMBER, IEEE, AND JOHN S. KOT

Abstract —As image line is an open waveguide, its finite, discrete spectrum of bound modes is complemented by a continuum. The latter plays an important role in discontinuity and radiation problems arising in circuit components and antenna applications. However, the continuous spectrum has failed to receive attention so far, possibly because of the essential two-dimensional, nonseparable nature of the problem. In this paper, we derive from basic principles the complete orthonormalized spectrum, under LSE/LSM assumptions, by means of a method of "partial wave phase shifts." The results are applicable to radiation and discontinuity problems in image line.

I. Introduction

IMAGE LINE is a structure of considerable theoretical interest, not only on its own merits, but also as a basic example of open waveguide of two-dimensional, nonseparable cross section [1].

Not surprisingly, the bound modes of image line have received considerable attention, and have been the object of numerical [2] and analytical treatment [3], by enclosing the guide in walls "far removed" [4] and retaining the open waveguide configuration [5]. It is fair to say that accurate results for the bound (discrete) modes have now been obtained by all of the above methods. The germane problem of the "rib waveguide" is also relevant to the theory (see [6], for instance).

Image line, however, is an open waveguide and consequently its spectrum includes a continuous range of modes. Excitation of the latter takes place due to discontinuities, such as steps, gaps, and bends, or when perturbations are located close to the air–dielectric interface, such as metal strips and radiating dipoles, if image line is to be used as a leaky-wave antenna [7]–[9]. Therefore, with a view to analyzing practical components, it is necessary to obtain a complete spectral characterization, inclusive of the continuum.

Once the complete spectrum is found, it is possible to construct the appropriate Green's function of the guide for use in the treatment of discontinuity problems. As stated above, the discrete components can be found by a variety of methods. Once found, they can be normalized over the two-dimensional cross section, if need be, numerically. The continuum, however, is not known and, moreover, its orthonormalization poses an interesting problem.

Manuscript received June 1, 1988; revised December 8, 1988.
T. Rozzi is with the School of Electrical Engineering, University of Bath, Bath, U.K.
J. S. Kot was with the School of Electrical Engineering, University of Bath, Bath, U.K. He is now with the Division of Radiophysics, CSIRO, Epping, N.S.W., Australia.
IEEE Log Number 8926583.

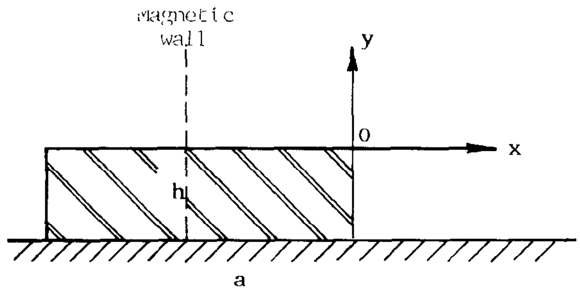

Fig. 1. Image line cross section (even E_y modes).

The task of normalizing the continuum is already nontrivial and tedious for one-dimensional multilayer guides. In image line, the problem is essentially complicated by the nonseparable nature of the problem, caused by the presence of the 90° diffraction edges (the dielectric corners), near which the transverse field becomes singular [10]. It is the very presence of these corners that causes the discrete modes to be essentially hybrid. The hybrid content, however, decreases very rapidly with aspect ratio (h/a—see Fig. 1) so that the much simpler pure LSM/LSE approximation does apply very well down to and close to the dielectric cutoff, for all aspect ratios smaller than unity, provided, that is, the edge conditions are still accounted for in the field distribution [11].

It is explicitly noted at this point that each discrete mode, existing as an independent field structure, must individually satisfy all boundary and edge conditions. Hence they need to be hybrid in general. A component of the continuum which cannot be excited individually is not so restricted; simple continuity (not analyticity) at the dielectric interfaces, excluding corners, is all that is required. The global continuum (radiative and nonradiative) will satisfy all the required conditions. In particular, a component of the continuum need not be hybrid, and a globally hybrid radiation field can be represented by a superposition of LSE and LSM radiation modes.

For the one-dimensional multilayer slab case, an elegant method, based on the transverse equivalent circuit interpretation and formal properties of the transverse Green's function, can be found in a textbook such as [12]. A clear treatment of the mathematical foundation of the process is, in fact, to be found in [13]. The extension to a *separable* two-dimensional cross section follows directly from the standard properties of Fourier integrals. The *nonseparable* two-dimensional problem is complicated as mentioned be-

0018-9480/89/0500-0868$01.00

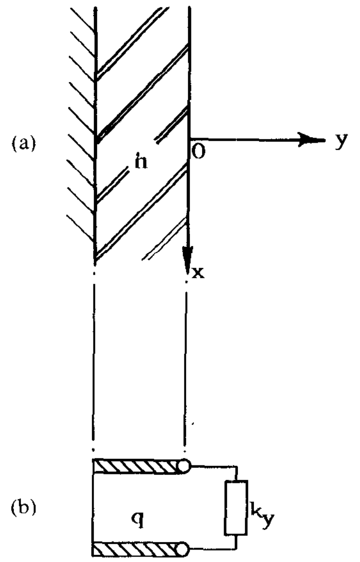

Fig. 2. Transverse equivalent circuit of a grounded slab.

fore, and does not seem, so far, to have drawn the attention of the applied mathematicians. In [14], a technique based on a transverse equivalent network of the "Hilbert" type was first introduced for the inset guide. There the geometry separates conveniently into a free-space region and a homogeneously filled slot region with discrete spectrum.

This is not the case for image line, but the basic concept still applies. In physical terms, this is tantamount to considering the scattering of each partial wave of the air region of Fig. 1 at the discontinuous interface $x = 0$ into the full spectrum of the slab region and recombining the individual contributions into an overall "phase shift" for the impinging partial wave. The result of this procedure is that the "shifted" partial waves are orthonormalized to a delta function of the transverse wavenumber $\underline{k}_t = (k_x, k_y)$ that identifies each partial wave in the air region.

In this contribution, the analysis will be developed for the even LSM (TM^y) polarization, having $H_y = 0$ and E_y as the main electric field component, whereas the LSE analysis proceeds along dual lines. An arbitrary radiation field can be described as a superposition of the LSM and LSE continua, as described above.

II. The Normalized Spectrum of the Slab Waveguide

The limiting case of the image guide for small aspect ratio is a dielectric slab over a ground plane. Inasmuch as the normalized complete spectrum of the grounded slab, illustrated in Fig. 2(a), and some of the concepts and notations used in deriving it will be required in the following development, it is useful to retrace briefly the steps involved. A detailed discussion can be found in [12].

If the expansion of the field takes place in terms of the transverse wavenumber in the air region, k_y, taken as an independent quantity, the wavenumber in the z direction, β, is determined by

$$\beta^2 = k_0^2 - k_y^2. \tag{1}$$

The completeness of the TM spectrum of the slab can then be stated as

$$\sum_s \varphi_s(y)\varphi_s(y') + \int_0^\infty dk_y\, \varphi(y;k_y)\varphi(y';k_y) = \epsilon_r(y)\delta(y-y') \tag{2}$$

where the summation is over the finite number of surface waves, the integral is over the continuum, and the orthonormalization is such that

$$\int_{-h}^{\infty} \frac{dy}{\epsilon_r(y)} \varphi_s(y)\varphi_r(y) = \delta_{sr} \tag{3a}$$

$$\int_{-h}^{\infty} \frac{dy}{\epsilon_r(y)} \varphi_s(y)\varphi(y;k_y) = 0 \tag{3b}$$

$$\int_{-h}^{\infty} \frac{dy}{\epsilon_r(y)} \varphi(y;k_y)\varphi(y;k_y') = \delta(k_y - k_y'). \tag{3c}$$

It is a well-known general property of the Sturm–Liouville equation, in this case the transmission line equation for propagation in the y direction, that the Green's function integrated over a path C in the complex k_y^2 plane to include all singularities yields the delta function. The singularities are constituted by the set of discrete poles, corresponding to the discrete spectrum, and branch line corresponding to the continuum, namely

$$-\frac{1}{2\pi j}\int_c g(y, y'; k_y^2)\, dk_y^2 = \epsilon_r(y)\,\delta(y-y'). \tag{4}$$

The Green's function g is constructed from two independent solutions of the transverse transmission line equation:

$$\overleftarrow{I} = \frac{\cos k(y+h)}{\cos kh} \tag{5a}$$

where

$$k^2 = \epsilon_r k_0^2 - \beta^2 = k_y^2 + (\epsilon_r - 1)k_0^2 \equiv k_y^2 + v^2 \tag{5b}$$

satisfying the boundary conditions for $y < 0$ and

$$\overrightarrow{I} = e^{-jk_y y} \tag{6}$$

satisfying the boundary conditions for $y > 0$ such that

$$\overleftarrow{I} = \overrightarrow{I} = 1 \quad \text{at} \quad y = 0. \tag{7}$$

We have then

$$g = \frac{\overleftarrow{I}(y;k_y^2)\overrightarrow{I}(y';k_y^2)}{j\omega\epsilon_0 Z(k_y^2)} \tag{8}$$

where Z is the total of the transverse equivalent circuit of Fig. 2(b) (the Wronskian of the transmission line equation which is independent of position):

$$\omega\epsilon_0 Z = k_y - \frac{jk}{\epsilon_r}\tan kh. \tag{9}$$

It is noted for future use that, with the above choice of voltage amplitudes, Z represents also the complex power of the transverse equivalent circuit.

It can also be seen that the occurrence of a pole of g in the complex k_y^2 plane at $k_y^2 = k_s^2$, say, coincides with the vanishing of the total susceptance of the transverse equivalent network. In order to recover (2) from (4), it is then sufficient to isolate the residues of the poles and modify the integration path so as to go *around* the branch line in the k_y^2 plane, by which process (4) can be rewritten, using (5) and (6), as

$$\sum_s \frac{\overleftarrow{I}(y; k_{ys}^2)\overrightarrow{I}(y'; k_{ys}^2)}{-j\omega\epsilon_0 \frac{\partial Z}{\partial ky^2}\Big|_{k_s^2}} + \frac{2}{\pi}\int_0^\infty dk_y k_y \operatorname{Im}\frac{\overleftarrow{I}(y; k_y)\overrightarrow{I}(y'; k_y)}{-j\omega\epsilon_0 Z(k_y)}$$

$$\equiv \sum_s \varphi_s(y)\varphi_s(y') + \int_0^\infty dk_y \varphi(y; k_y)\varphi(y'; k_y). \quad (10)$$

In (10), it is then possible to make the identification

$$\varphi_s(y) = \frac{\overleftarrow{I}(y; k_{ys}^2)}{\left[-j\omega\epsilon_0 \frac{\partial Z}{\partial k_y^2}\Big|_{k_s^2}\right]^{1/2}}, \qquad y < 0 \quad (11)$$

and similarly for $y > 0$, yielding the well-known expressions for the TM surface wave of a grounded slab:

$$\varphi_s(y) = A_s \frac{\cos k_s(y+h)}{\cos k_s h}, \qquad y \leqslant 0 \quad (12a)$$

$$= A_s e^{-\gamma_s y}, \qquad y \geqslant 0 \quad (12b)$$

with

$$A_s = \left\{ \frac{2\epsilon_r}{h + \frac{\epsilon_r}{\gamma_s}\left[1 + \frac{\gamma_s^2}{k_s^2}(1+\epsilon_r\gamma_s h)\right]} \right\}^{1/2}$$

$$\gamma_s - \frac{k_s}{\epsilon_r}\tan k_s h = 0. \quad (13)$$

A substantially analogous procedure leads to the determination of the component of the continuum $\varphi(y, k_y)$.

Let us introduce in (9) the following quantity of convenience:

$$\tan\tilde{\alpha} = \frac{k}{k_y \epsilon_r}\tan kh \quad (14)$$

and substitute (14) in (8). The resulting expression for a component of the continuum corresponding to the value k_y, $0 \leqslant k_y < \infty$, of the y wavenumber is then

$$\varphi(y : k_y) = \sqrt{\frac{2}{\pi}}\cos\tilde{\alpha}\frac{\cos k(y+h)}{\cos kh}, \qquad y \leqslant 0 \quad (15a)$$

$$= \sqrt{\frac{2}{\pi}}\cos(k_y y + \tilde{\alpha}), \qquad y \geqslant 0 \quad (15b)$$

which satisfies implicitly the orthonormalization conditions (3). It is noted that the angle $\tilde{\alpha}$ above represents, in fact, the phase shift a ray with propagation constant (k_y, β) undergoes upon impinging on the slab and reemerging from it.

III. Discrete Spectrum of Image Guide—LSM Formulation

From a y-directed electric Hertzian potential $\underline{\Pi}e = \hat{y}\psi(x, y)e^{-j\beta z}$, the following field components are recovered:

$$\begin{aligned} &E_x = \partial_x \partial_y \psi_e \qquad E_y = \epsilon_r k_0^2 + \partial_y^2 \psi_e \\ &E_z = -j\beta\partial_y\Psi_e \\ &H_x = -\omega\epsilon\beta\psi_e \qquad H_y = 0 \\ &H_z = j\omega\epsilon\partial_x\psi_e. \end{aligned} \quad (16)$$

Considering that we have chosen to view the plane $x = 0$ as the discontinuous interface, that the field is TE to x, and that we want to keep the transverse electric field singular at the corner as the unknown, we shall proceed with an admittance formulation in terms of the pair E_y, H_z. Hence, for a plane traveling wave in air with x-directed wavenumber k_x, the modal admittance is

$$Y_0 = \frac{H_z}{E_y} = \frac{k_y}{\omega\mu_0} \quad (17)$$

while for a short-circuited section of length a and x-directed wavenumber q the driving point admittance is

$$Y_s = j\frac{q}{\omega\mu_0}\tan qa. \quad (18)$$

Assuming an even symmetry in x of ψ_e, E_y, and H_z, the field E_y of a bound mode in the region $x \geqslant 0$ is describable as

$$E_y(x, y) = \int_0^\infty dk_y \tilde{V}(k_y)\sqrt{\frac{2}{\pi}}\cos k_y(y+h)\bar{e}^{|k_x|x} \equiv \psi_s(x, y) \quad (19)$$

with

$$k_x^2 = k_0^2 - \beta_s^2 - k_y^2 \equiv k_t^2 - k_y^2 < 0$$

as for a bound mode $k_t^2 < 0$.

In the region $x \leqslant 0$, we have

$$\psi_s(x, y) = V_s\frac{\varphi_s(y)}{\epsilon_r(y)}\chi_s(x) + \int_0^\infty d\rho V'(\rho)\frac{\varphi(y, \rho)}{\epsilon_r(y)}\chi(x) \quad (20)$$

where $\varphi_s(y)$ is the normalized distribution of a TM surface wave of the slab, considered monomode, and $\varphi(y, \rho)$ is that of its continuum. Moreover

$$\chi_s(x) = \frac{\cos q_s(x+a)}{\cos q_s a} \quad (21)$$

with

$$q_s^2 = \epsilon_r k_0^2 - \beta_s^2 - k_s^2 = k_0^2 - \beta_s^2 + \gamma_s^2$$
$$q^2 = k_0^2 - \beta_s^2 - \rho^2 \tag{22}$$

k_s being the y-directed wavenumber of the slab surface wave in the dielectric ($|y| \leqslant -h$) and γ the decay constant in air ($y \geqslant 0$). The amplitudes $\tilde{V}(k_y), V_s, V'(\rho)$ of the spectral components of E_y and the corresponding ones of H_z are related by (1).

For a bound mode ($\beta_s > k_0$), q is pure imaginary but χ remains real. For real $q(\beta_s \leqslant k_0)$, poles of χ occur at $qa = n\pi/2$, $n = 1,3,5 \cdots$, when the open-circuit stub corresponding to the slab region is resonant. At these values of ρ_n, however, a short circuit appears at $x = 0$, where $\chi = 1$, and the regions to the left and the right of the interface are decoupled. In order not to violate the boundary conditions on E_y, their contributions to the ρ integral must vanish; hence $V(\rho_n') \to 0$ sufficiently fast for this to happen and the integral in (20) must be identified with its principal value ($⨍$).

By utilizing the continuity of H_z, E_y at $x = 0$ it is then possible to eliminate the amplitudes $\tilde{V}, V_s, V'$ and establish the usual integral equation for the unknown field $E(y) \equiv E_y(0, y)$, namely,

$$\int_{-h}^{\infty} (G_s + G_a + G_s') E \, dy = 0 \tag{23}$$

where we have introduced the following quantities:

$$G_s = j\omega\epsilon_0 q_s \frac{\tan q_s a}{q_s^2 + \beta_s^2} \varphi_s(y) \varphi_s(y') \tag{24a}$$

$$G_a(y, y') = j\omega\epsilon_0 \frac{2}{\pi} ⨍_0^{\infty} dk_y \frac{\sqrt{k_t^2 - k_y^2}}{k_0^2 - k_y^2} \cos k_y y \cos k_y y' \tag{24b}$$

$$G_s'(y, y') = j\omega\epsilon_0 ⨍_0^{\infty} d\rho \frac{q \tan qa}{k_0^2 - \rho^2} \varphi(y, \rho) \varphi(y', \rho). \tag{24c}$$

We multiply on the left by $E(y)$, integrate over y, and divide by $\langle E, \varphi_s \rangle^2$, where the bracket notation denotes integration over y. The following scalar dispersion equation is obtained, which is illustrated by the equivalent circuit of Fig. 3:

$$Y_s + Y_a + Y_s' = 0 \tag{25}$$

where

$$Y_s = j\omega\epsilon_0 \frac{q_s \tan q_s a}{q_s^2 + \beta_s^2} \tag{26a}$$

$$Y_a = \frac{\langle E, G_a, E \rangle}{\langle E, \varphi_s \rangle^2} \tag{26b}$$

$$Y_s' = \frac{\langle E, G_s', E \rangle}{\langle E, \varphi_s \rangle^2}. \tag{26c}$$

Y_s is the driving point admittance seen by the slab surface wave, Y_a that of the air region, and Y_s' that of the continuous spectrum of the slab.

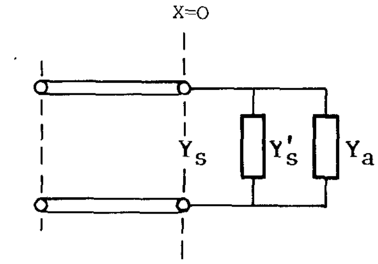

Fig 3. Equivalent circuit for transverse resonance equation (26).

It is noted that

i) Y_a and Y_s' are pure imaginary, for, even when q is pure imaginary, we still have
$$q \tan qa = -|q| \tanh |q| a.$$
ii) The Green's functions G_a and G_s' contain principal value integrals. Poles of the tan function, arising from χ_s, have been excluded before. Simple poles occur also at $k_y = k_0$ in (24b) and at $\rho = k_0$ in (24c). At these points, however, owing to (16), we have $\tilde{V}(k_0) = V'(k_0) = 0$.
iii) Y_a and Y_s, the admittances in (25), are functions of the unknown β_s. The latter is determined by solving for β_s the dispersion equation (25).

Once β_s is found, the field components are determined from the potential. The required normalization is according to

$$\int_{-a}^{\infty} dx \int_{-h}^{\infty} dy \, \psi^2(x, y) = 1 \tag{27}$$

where it is noted that a weight factor $1/\epsilon_r$ is already built in (2).

Although the normalization constant can be found by direct integration, it is more effective to use the equivalent circuit of Fig. 3 by recognizing that the residue of (26) at resonance fixes V_s, and consequently all other amplitudes, in such a manner that (27) is satisfied, namely

$$V_s^{-2} = j\omega\epsilon_0 \frac{\partial}{\partial k_t^2} Y(k_t^2 = k_{ts}^2).$$

IV. The Continuous Spectrum of Image Line

This portion of the spectrum was never investigated before. As the cross section is two-dimensional, it is apparent that an expansion of the continuum must be written in terms of two independent wavenumbers, the third being fixed by the wave equation. We choose $(k_x, k_y) = \underline{k}_t$ as the two independent quantities in the air region and, correspondingly, develop the field in the air region in terms of partial waves of the type

$$\sqrt{\frac{2}{\pi}} \cos(k_x x + \alpha) \sqrt{\frac{2}{\pi}} \cos k_y (y + h).$$

It is noted, however, that the "phase shift" α is now a function of *both* k_x and k_y because of the nonseparability.

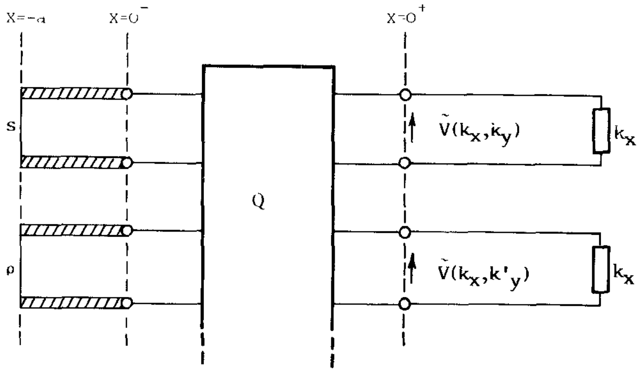

Fig. 4. Multiport equivalent circuit for a component of the continuum

It is noted that as the transverse Green's admittance function (8) only contains $k_y^2(k_x^2)$, k_x, k_y can be limited to the interval $0 \leqslant k_x, k_y < \infty$. This is a consequence of choosing to represent the continuum by a set of standing waves.

We require that the components of the continuum satisfy the orthogonality condition over the guide cross section S:

$$\iint_S \psi(x, y; k_x, k_y)\psi(x, y: k_x', k_y')\,dx\,dy = \delta(k_x - k_x')\,\delta(k_y - k_y') \equiv \delta(\underline{k}_t - \underline{k}_t'). \quad (28)$$

This fact imposes a generalization on the concept of the scalar transverse impedance we met in the previous sections as follows.

The transverse equivalent circuit appropriate to the new situation is shown in Fig. 4. The discontinuous interface $x = 0$ acts as an ideal transformer coupling slab components with a different wavenumber k_s, ρ and partial waves in air with different wavenumber k_y.

We shall now generalize the method described in Section II. This involves constructing the transverse Green's function from an outward and an inward traveling wave at the interface $x = 0$.

An outward travelling partial wave in the air region with wavenumber $\underline{k}_t$ and Fourier amplitude $\tilde{V}(\underline{k}_t)$ is expressed as

$$\vec{V}(x, y; \underline{k}_t) = \sqrt{\frac{2}{\pi}}\,\tilde{V}(\underline{k}_t)\cos k_y(y+h)e^{-jk_x x}. \quad (29)$$

Correspondingly, there exists a standing wave in the slab region expressible as

$$\overleftarrow{V}(x, y; \underline{k}_t) = \left[Q_s(k_y)\chi_s(x)\varphi_s(y) + \int_0^\infty d\rho\, Q(k_y, \rho) \cdot \chi(x, \rho)\varphi(y, \rho)\right]\tilde{V}(\underline{k}_t). \quad (30)$$

The continuity equation that replaces (7) is now

$$\overleftarrow{V}(y, 0; \underline{k}_t) = \vec{V}(y, 0; \underline{k}_t) \quad (31)$$

which allows the coefficients $Q_s, Q(k_y, \rho)$ to be determined by orthogonality of the $\varphi_s, \varphi(\rho)$ as

$$Q_s(k_y) = \int_{-h}^{\infty}\sqrt{\frac{2}{\pi}}\cos k_y(y+h)\varphi_s(y)\,dy \quad (32a)$$

$$Q(k_y, \rho) = \int_{-h}^{\infty}\sqrt{\frac{2}{\pi}}\cos k_y(y+h)\varphi(y, \rho)\,dy \quad (32b)$$

given in (A8), Appendix II.

As a mathematical point, it is noted that the continuum constructed in the following from the above definition (32) of the transformer ratio will be automatically orthonormal, but it will only be orthogonal to the expression of the bound mode as assumed in (32a). Moreover, the coefficients $Q(k_y; \rho)$ are distributions. This is not surprising, inasmuch as the continuous modes are not square-integrable; nor do they satisfy the edge condition at the dielectric corners. This poses no real problems, inasmuch as the coefficients Q only appear under the integral sign. An alternative, better conditioned approach would be to expand the partial air waves and the slab spectrum at $x = 0$ in terms of an appropriate discrete set of expanding functions, possibly satisfying the edge condition, and then evaluate (32) in the transformed domain as the scalar products of the coefficients of the expansion.

The impedance looking into the slab region, as seen from the reference planes at $x = 0^-$, is given by the parallel combination of the admittance of transmission lines, each corresponding to a spectral component of the slab, terminated by a short circuit at $x = -a$. This circuit is embedded in the transformer Q (see Fig. 4) so that at $x = 0^+$, we have

$$\omega\epsilon_0\overleftarrow{Y}(k_y, k_y') = jq_s \tan q_s a Q_s(k_y)Q_s(k_y') + j\int_0^\infty d\rho\, q(\rho)\tan q(\rho)a \cdot Q(k_y; \rho)Q(k_y', \rho) \quad (33)$$

where now

$$q_s^2 = (\epsilon_0 - 1)k_0^2 + k_t^2 - k_s^2 \qquad q^2 = k_t^2 - \rho^2. \quad (34)$$

In the air region, two different components k_y and k_y' do not couple and a component with x-directed wavenumber k_x propagates in the positive x direction with a characteristic admittance $k_x/\omega\epsilon_0$. Hence the admittance of the air region, in the representation of the partial waves, is a discrete function of k_y with amplitude k_x, namely

$$\omega\mu_0\vec{Y}(k_y, k'y) = k_x\delta(k_y - k_y') \quad (35)$$

with

$$Y(k_y, k_y') = \overleftarrow{Y} + \vec{Y} \equiv jB(k_y, k_y').$$

The complex power (times $-j\omega\mu_0$) corresponding to the component $\underline{k}_t = (k_x, k_y)$ is given by

$$P(\underline{k}_t) = \omega\mu_0\tilde{V}(\underline{k}_t)\int_0^\infty B(k_y, k'y)\tilde{V}(k_x, k_y')\,dk_y'. \quad (36)$$

If $V(\underline{k}_t)$ is set equal to unity in (29), from (33), (35), and

(36), we have

$$p = \frac{1}{j} k_x + q_s \tan q_s a \, Q_s(k_y) J_s + \int_0^\infty d\rho \, q(\rho) \tan q(\rho) a \, Q(k_y, \rho) J(\rho) \quad (37)$$

where

$$J_s = \int_0^\infty dk_y Q_s(k_y) = \sqrt{\frac{\pi}{2}} \frac{A_s}{\cos k_s h} \quad (38a)$$

and

$$J(\rho) = \int_0^\infty dk_y Q(k_y, \rho) = \frac{\cos \tilde{\alpha}}{\cos kh} + \cos(\rho h - \tilde{\alpha}) \quad (38b)$$

are derived in Appendix II (eq.(A9)).

In the following, for the sake of compactness, we shall write the second and third terms in (37) together as

$$\sum_n q_n \tan q_n a \, Q_n(k_y) J_n$$

where n now stands for a component, discrete or continuous, of the spectrum and the summation for a discrete sum or integral over ρ; correspondingly, $\varphi_n(y)$ denotes the slab modal distribution. It is again useful to define a "phase shift" $\alpha(\underline{k}_t)$ such that

$$\tan \alpha = \frac{1}{k_x} \sum_n q_n \tan q_n a \, Q_n J_n. \quad (39)$$

Using (39) in (10) we have

$$\frac{2}{\pi} k_x \mathrm{Re}\left[\frac{\overleftarrow{V}(x)\vec{V}(x', y'; \underline{k}_t)}{k_x + jk_x \tan \alpha}\right] = \sqrt{\frac{2}{\pi}} \sum_n Q_n \chi_n(x) \varphi_n(y) \cos \alpha \cdot \frac{2}{\pi} \cos k_y(y' + h) \cos(k_x x' + \alpha) \equiv \psi(x, y; \underline{k}_t) \psi(x', y'; \underline{k}_t) \quad (40)$$

from which the components of the continuum can be identified as

$$\psi(x, y; k_t) = \sqrt{\frac{2}{\pi}} \cos \alpha \sum_n Q_n \chi_n(x) \varphi_n(y), \qquad x \leqslant 0$$
$$= \frac{2}{\pi} \cos k_y(y + h) \cos(k_x x + \alpha), \qquad x \geqslant 0. \quad (41)$$

In Appendix I it is verified by direct integration that the orthonormalization condition (28) is indeed satisfied by (41).

Appendix I
Direct Check on Orthonormality of the Continuum

We want to verify that the condition

$$\iint_S dx\, dy\, \psi(x, y; \underline{k}_t) \psi(x, y; \underline{k}_t) = \delta(\underline{k}_t - \underline{k}_t') \quad (A1)$$

is satisfied by direct integration.

Define I_1 as the integration over the slab region. This is given by

$$I_1 = \int_{-h}^\infty dy \int_{-a}^0 dx \sum_n Q_n(k_y) Q_n(k_y') \cos \alpha \cos \alpha' \cdot \varphi_n(y) \varphi_n'(y) \frac{2}{\pi} \frac{\cos q_n(x + a)}{\cos q_n a} \cdot \frac{\cos q_n'(x + a)}{\cos q_n' a} \quad (A2)$$

where

$$\alpha' = \alpha(k_x', k_y') \qquad q_n^2 = k_t^2 - k_n^2.$$

The quantity k_n denotes either the y-directed wavenumber of the slab surface wave in air, $-j\gamma_s$, or the continuous wavenumber ρ.

By orthogonality of the φ_n and integration over x, we have

$$I_1 = \sum_n Q_n(k_y) Q_n(k_y') \cdot \frac{\cos \alpha}{\cos q_n a} \cdot \frac{\cos \alpha}{\cos q_n' a} \cdot \frac{1}{\pi} \cdot \left[\frac{\sin(q_n - q_n')a}{q_n - q_n'} + \frac{\sin(q_n + q_n')a}{q_n + q_n'}\right]$$
$$= \frac{2}{\pi} \frac{\cos \alpha \cos \alpha'}{k_t^2 - k_t'^2} \sum_n Q_n(k_y) Q_n(k_y') \cdot (q_n \tan q_n a - q_n' \tan q_n' a). \quad (A3)$$

In the air region, we have

$$I_2 = \int_0^\infty dx \int_{-h}^\infty dy \frac{2}{\pi} \cos k_y(y + h) \cos k_y'(y + h) \cdot \frac{2}{\pi} \cos(k_x x + \alpha) \cos(k_x' x + \alpha')$$
$$= \delta(k_y - k_y') \left\{\delta(k_x - k_x') \cdot -\frac{1}{\pi}\left[\frac{\sin(\alpha - \alpha')}{k_x - k_x'} + \frac{\sin(\alpha + \alpha')}{k_x + k_x'}\right]\right\}$$
$$= \delta(k_y - k_y') \left\{\delta(k_x - k_x') - \frac{2}{\pi} \frac{\cos \alpha \cos \alpha'}{k_x^2 - (k_x')^2} \cdot (k_x \tan \alpha - k_x' \tan \alpha')\right\}. \quad (A4)$$

Satisfaction of (A1) requires

$$I_1 + I_2 = \delta(k_x - k_x') \delta(k_y - k_y'). \quad (A5)$$

If a second term in (A4) equals I_1, this is indeed the case. It is now verifiable that (A5) holds provided α is chosen such that

$$k_x \tan \alpha \, \delta(k_y - k_y') = \sum_n Q_n(k_y) Q_n(k_y') q_n \tan q_n a. \quad (A6)$$

Integrating with respect to k_y' from 0 to ∞, we recover

$$k_x \tan \alpha = \sum_n J_s Q_n(k_y) q_n \tan q_n a \quad (A7)$$

which is just our definition (39) of α.

Appendix II

In (32a), Q_s is in fact the Fourier transform of φ_s. This is given by [15, p. 477]

$$Q_s(ky) \equiv \tilde{\varphi}_s(k_y)\frac{A_s}{\sqrt{2\pi}}\left\{\frac{2}{\gamma_s^2+k_y^2}\left[\gamma_s\cos k_y h - k_y\sin k_y h\right] + \frac{1}{\cos k_s h}\left[\frac{\sin(k_s+k_y)h}{k_s+k_y}+\frac{\sin(k_s-k_y)h}{k_s-k_y}\right]\right\}. \qquad \text{(A8a)}$$

In (32b),

$$\begin{aligned} Q(k_y,\rho) &= \tilde{\varphi}(k_y) \\ &= \frac{1}{\pi}\frac{\cos\tilde{\alpha}}{\cos kh}\left[\frac{\sin(k+k_y)h}{k+k_y} + \frac{\sin(k-k_y)h}{k-k_y}\right] \\ &\quad + \cos(k_y h - \tilde{\alpha})\,\delta(k_y-\rho). \end{aligned} \qquad \text{(A8b)}$$

In evaluating

$$J_s = \int_0^\infty dk_y\, Q_s(k_y) \qquad \text{(A9a)}$$

from (A8a), we realize that

$$\sum_{\pm}\int_0^\infty \frac{\sin(k_s \pm k_y)h}{k_s \pm k_y}\,dk_y = \int_{-\infty}^{+\infty}\frac{\sin(k_s+k_y)}{k_s+k_y}\,dk_y = \pi$$

and that the first square bracket term in (A8a) integrates to zero [15, p. 406]. Hence, we obtain

$$J_s = \sqrt{\frac{\pi}{2}}\,\frac{A_s}{\cos k_s h}.$$

Similarly, in (38b), we obtain

$$\begin{aligned} J(\rho) &= \int_0^\infty dk_y\, Q(k_y,\rho) \\ &= \frac{\cos\alpha}{\cos kh} + \cos(\rho h - \tilde{\alpha}). \end{aligned} \qquad \text{(A9b)}$$

References

[1] R. M. Knox, "Dielectric waveguide integrated circuits—An overview," *IEEE Trans. Microwave Theory Tech.*, vol. MTT-24, pp. 806–814, Nov. 1976.

[2] K. Hayata, M. Koshiba, M. Eguchi, and M. Suzuki, "Vectorial finite-element method without any spurious solutions for dielectric waveguiding problems using transverse magnetic-field component," *IEEE Trans. Microwave Theory Tech.*, vol. MTT-34, pp. 1120–1124, Nov. 1986.

[3] R. Mittra, Y. L. Hou, and V. Jamnejad, "Analysis of open dielectric waveguides using mode matching technique and variational methods," *IEEE Trans. Microwave Theory Tech.*, vol. MTT-28, pp. 36–43, Jan. 1980.

[4] S. T. Peng, A. A. Oliner, T. I. Hsu, and A. Sanchez, "Guidance and leakage properties of a class of open dielectric waveguide," (Part I and II), *IEEE Trans. Microwave Theory Tech.*, vol. MTT-29, pp. 843–869, Sept. 1981.

[5] J. S. Kot and T. Rozzi, "Rigorous modelling of single and coupled image and insular waveguide by transverse resonance diffraction," in *Proc. 14th European Microwave Conf.* (Liege), Sept. 1984, pp. 424–429.

[6] N. Dagli and C. G. Fonstad, "Universal design curves for rib waveguides," *J. Lightwave Technol.*, vol. 6, pp. 1136–1145, June 1988.

[7] R. Mittra and R. Kastner, "A spectral domain approach for computing the radiation characteristics of a leaky wave antenna for millimetre waves," *IEEE Trans. Antennas Propagat.*, vol. AP-29, pp. 652–654, July 1981.

[8] T. Itoh, "Application of gratings in a dielectric waveguide for leaky wave antennas and band-reject filters," *IEEE Trans. Microwave Theory Tech.*, vol. MTT-25, pp. 1134–1138, Dec. 1977.

[9] K. L. Klohn, R. E. Horn, H. Jacobs, and E. Freibergs, "Silicon waveguide frequency scanning linear array antenna," *IEEE Trans. Microwave Theory Tech.*, vol. MTT-26, pp. 764–773, Oct. 1978.

[10] J. Bach Andersen and V. V. Solodukhov, "Field behaviour near a dielectric wedge," *IEEE Trans. Antennas Propagat.*, vol. AP-26, pp. 598–602, July 1978.

[11] T. Rozzi and S. Hedges, "Rigorous analysis and network modelling of the inset dielectric guide," *IEEE Trans. Microwave Theory Tech.*, vol. MTT-35, pp. 823–834, Sept. 1987.

[12] N. Marcuvitz and L. Felsen, *Radiation and Scattering of Waves*. Englewood Cliffs, NJ: Prentice Hall, 1973, ch. 3, pp. 278–282.

[13] B. Friedman, *Principles and Techniques of Applied Mathematics*. New York: Wiley, 1956, ch. 4.

[14] T. Rozzi and L. Ma, "Mode completeness, normalization and Green's function of the inset dielectric guide," *IEEE Trans. Microwave Theory Tech.*, vol. 36, pp. 542–551, Mar. 1988.

[15] I. S. Gradshteyn and I. M. Ryzhik, *Table of Integrals, Series and Products*. New York: Academic Press, 1980.

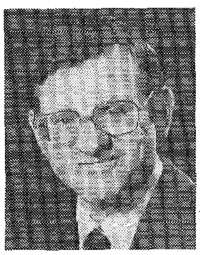

Tullio Rozzi (M'66–SM'74) obtained the degree of 'Dottore' in physics from the University of Pisa in 1965 and the Ph.D. degree in electronic engineering at Leeds University in 1968. In June 1987 he received the degree of D.Sc. from the University of Bath, Bath, England.

From 1968 to 1978 he was a Research Scientist at the Philips Research Laboratories, Eindhoven, the Netherlands, having spent one year, 1975, at the Antenna Laboratory, University of Illinois, Urbana. In 1975 he ws awarded the Microwave Prize of the Microwave Theory and Technique Group of the Institute of Electrical and Electronics Engineers. In 1978 he was appointed to the Chair of Electrical Engineering at the University of Liverpool and subsequently was appointed to the Chair of Electronics and Head of the Electronics Group at the University of Bath in 1981. From 1983 to 1986 he held the additional responsibility of Head of the School of Electrical Engineering at Bath. Since 1986 Dr. Rozzi has also held the 'ordinary chair' of Antennas at the Faculty of Engineering, University of Ancona, Italy.

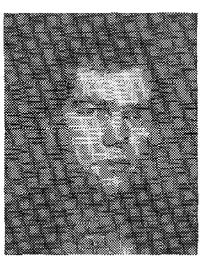

John S. Kot obtained the B.Eng. degree in electrical engineering from the University of Liverpool, Liverpool, England, in 1981 and the Ph.D. degree, also in electrical engineering, from the University of Bath, Bath, England, in 1984.

From 1984 to 1988 he was a Research Officer in the Electrical Engineering Department at Bath University, working in the area of microwave and millimeter-wave components, in particular, the dielectric waveguide. He is currently a member of staff of CSIRO, Division of Radiophysics, Epping, New South Wales, Australia.